Structure of the Extracellular Domain of Human Tissue Factor: Location of the Factor VIIa Binding Site‡

Yves A. Muller, Mark H. Ultsch, Robert F. Kelley, and Abraham M. de Vos*

Department of Protein Engineering, Genentech, Inc., 460 Point San Bruno Boulevard, South San Francisco, California 94080

Received June 20, 1994; Revised Manuscript Received July 13, 1994•

ABSTRACT: Tissue factor, the obligate cofactor for coagulation factor VII, plays an essential role in hemostasis by initiating the extrinsic pathway of blood coagulation upon vascular damage, making it a promising target for new anticoagulant therapies in the treatment of thrombosis and sepsis. The three-dimensional structure of the extracellular domain of tissue factor, determined by X-ray crystallography at a resolution of 2.4 Å, consists of two domains of approximately equal size, with a topology characteristic of fibronectin type III modules. Comparison of tissue factor with the extracellular domain of the growth hormone receptor, which belongs to the same receptor superfamily, shows that the relative orientation between these domains as well as the domain–domain interface is very different. These differences have dramatic consequences for the residues in tissue factor that are homologous to the binding determinants of the growth hormone receptor. Alanine-scanning mutagenesis has identified tissue factor residues important for factor VIIa binding. The structure shows that the binding site is located in the domain–domain interface region but on the opposite side of the molecule compared to the growth hormone receptor, with the binding determinants residing on β-strands rather than on loops.

Tissue factor is the principal initiator of the vertebrate coagulation cascade (Nemerson, 1988; Davie et al., 1991; Ruf & Edgington, 1994). TF[1] is an integral membrane glycoprotein (263 residues) consisting of an extracellular part (residues 1–219), a single membrane-spanning region (residues 220–242), and a small cytoplasmic domain (residues 243–263) (Morrissey et al., 1987; Scarpati et al., 1987; Spicer et al., 1987) and is expressed on cells of the tissue adventitia (Wilcox et al., 1989). Vascular damage exposes blood to cells expressing TF, which forms a calcium-dependent, high-affinity complex with plasma factor VII (FVII). Binding to TF promotes activation of zymogen FVII to the serine protease FVIIa (Nemerson & Repke, 1985) through cleavage of the Arg152–Ile153 peptide bond catalyzed *in vitro* by a number of proteases. Activation *in vivo* may occur through an autocatalytic mechanism (Nakagaki et al., 1991; Neuenschwander et al., 1993). TF functions as an essential cofactor for FVIIa by dramatically enhancing the catalytic efficiency of FVIIa for both peptide (Lawson et al., 1992) and protein substrates (Bom & Bertina, 1990). The TF·FVIIa complex activates factors IX and X, ultimately resulting in thrombin generation and the formation of a fibrin clot.

On the basis of multiple sequence alignments of the extracellular segments, Bazan (1990) proposed that TF is a member of the cytokine receptor superfamily. On the basis of the distribution of cysteine residues, the members of this superfamily have been grouped in two classes. Class I consists of the human growth hormone receptor, the prolactin receptor, the erythropoietin receptor, and the interleukin 3 and interleukin 4 receptors, while class II includes TF and the interferon α and β receptors. The crystal structure of the human growth hormone receptor (De Vos et al., 1992) shows that the cytokine receptor extracellular part consists of two Ig-like domains with the ligand-binding site located at the domain–domain interface. Structure–function analysis of TF is required to address how the cytokine receptor fold is used as a cofactor for a serine protease.

TF is not normally expressed on cells within the vasculature but is found in artherosclerotic plaque (Wilcox et al., 1989) and can be induced on endothelial cells and monocytes by exposure to inflammatory cytokines or bacterial lipopolysaccharide (Gregory et al., 1989). Animal experiments with neutralizing antibodies suggest an important role for TF in the pathophysiology of thrombosis and sepsis. Anti-TF antibodies prevent death in a primate model of *Escherichia coli*-induced septic shock (Taylor et al., 1991), attenuate endotoxin-induced disseminated intravascular coagulation in rabbits (Warr et al., 1990), and inhibit thrombus formation in a rabbit model of arterial thrombosis (Pawashe et al., 1994). The structural analysis of TF will provide the basis for the design of drugs that modulate TF function, which could have important therapeutic applications in sepsis and thrombotic disorders. Here, we report the structure of the extracellular portion of human tissue factor determined at 2.4-Å resolution.

EXPERIMENTAL PROCEDURES

The extracellular portion (residues 1–219) of wild-type human TF and of two single-point mutants, selected on the basis of the structure of the human growth hormone receptor (Thr126 mutated to Cys and Thr154 to Cys), was expressed by secretion in *Escherichia coli* and purified to homogeneity by anion-exchange, hydrophobic-interaction, and size exclusion chromatography. Electrospray-ionization mass spectroscopy showed that this material had an N-terminal sequence and molecular weight consistent with those of mature TF(1–219), and FVIIa binding and cofactor function were consistent with those reported for soluble TF by Neuenschwander and Morrissey (1994). Crystals were grown by the sitting drop method, equilibrating a droplet of 50 μL of protein solution (23 mg/mL protein, 0.1 M sodium chloride, 1 mM PMSF, 20 mM TRIS, pH 7.5) mixed with 10 μL of reservoir solution

‡ The coordinates have been deposited with the Brookhaven Protein Data Bank (entry 1HFT).

* To whom correspondence should be addressed.

• Abstract published in *Advance ACS Abstracts*, August 15, 1994.

[1] Abbreviations: TF, tissue factor; FVII, factor VII; FVIIa, activated factor VII; PMSF, phenylmethanesulfonyl fluoride; Gla, γ-carboxyglutamic acid.

0006-2960/94/0433-10864$04.50/0

Table 1: Data Collection and Phasing Statistics

compound	resolution (Å)	observations (no.)	reflections (no.)	completeness (%)	R_{merge}[a] (%)	R_{scale}[b] (%)	phasing power
native 1[c]	15–3.0	42598	5294	96	5.7		
native 2[d]	30–2.4	36268	9132	88	7.5		
T154C[c]	15–4.0	6446	1887	77	3.9	13.5	1.66
T154C[c]	6.5–3.1	12240	3946	91	5.8	23.5	0.80
T126C[c]	15–4.0	6292	1899	78	4.3	24.9	0.92
T126C[e]	30–3.1	20212	3983	80	6.5	15.0	1.32
K_2PtCl_4[c]	15–4.0	8383	2155	88	4.3	25.1	1.09
K_2HgI_4[c]	15–4.0	6613	2096	86	3.6	20.4	1.01

[a] $R_{merge} = \Sigma\Sigma|I_i - \langle I\rangle|/\Sigma\Sigma I_i$. [b] $R_{scale} = \Sigma|F_{native} - F_{derivative}|/\Sigma F_{native}$. [c] Collected using a Rigaku rotating anode generator with Cu Kα radiation on an Enraf-Nonius FAST area detector and processed using MADNES (Messerschmidt & Plufgrath, 1987) and PROCOR (Kabsch, 1988). [d] Collected at CHESS, Cornell (λ = 0.908 Å), and processed with DENZO and SCALEPACK. [e] Collected on a MAR imaging plate using a Rigaku rotating anode generator with Cu Kα radiation and processed with XDS (Kabsch, 1988).

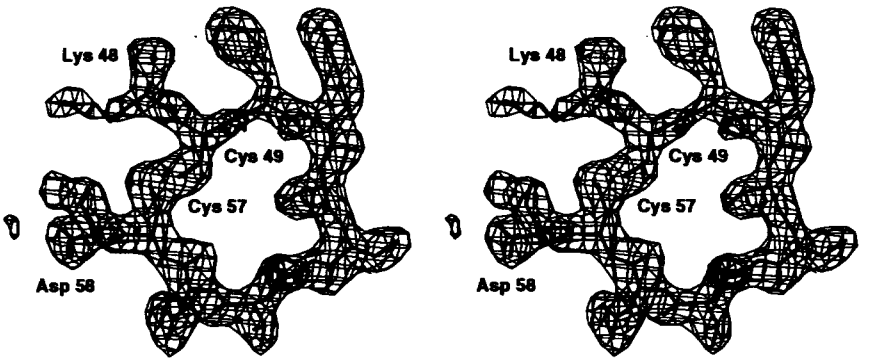

FIGURE 1: Region of the final electron density map with the model for segment Lys47–Asp58 superimposed, including the disulfide bond between Cys49 and Cys57. The density was calculated with coefficients $2F_o - F_c$ and contoured at 1.3σ; only density within 2.5 Å of the atomic positions is displayed.

(50% saturated ammonium sulfate, 0.1 M TRIS, pH 7.5) against 30 mL of reservoir solution. Single, lens-shaped crystals grew within 3–4 weeks to an average size of 0.4 × 0.4 × 0.3 mm^3. The crystals were stored in a solution containing 60% saturated ammonium sulfate and 0.1 M TRIS, pH 7.5. The crystals belong to space group $P4_12_12$ with cell parameters a = 45.5 Å and c = 231.0 Å. Similar crystals of the extracellular portion of TF have been reported earlier, although they were grown under different conditions (Boys et al., 1993). The crystals diffract highly anisotropically with the diffraction pattern extending beyond 2.0-Å resolution along the crystallographic c^* axis but only to about 2.4 Å in the a^*/b^* plane.

The structure was solved by multiple isomorphous replacement, using a native data set to 3-Å resolution collected from four crystals and six heavy atom derivative data sets each collected from a single crystal (Table 1). An initial set of phases to 3.1-Å resolution was obtained using wild-type crystals soaked with K_2PtCl_4 or K_2HgI_4 and the two cysteine point mutants cocrystallized with methylmercury(II) iodide. Heavy atom positions were identified with the program HASSP (Terwilliger et al., 1987), and phase refinement was carried out with PROTEIN (Steigemann, 1974) including anomalous differences for several of the data sets. Solvent flattening according to Wang (1985) increased the figure of merit from 0.61 to 0.76. The program FRODO (Jones, 1978) was used for model building. The interpretation of the map was corroborated by the positions of the cysteine mutations, the heavy atom sites, and the two disulfide bridges, as well as the unambiguous assignment of bulky side chains. A second native data set to 2.4-Å resolution was collected from eight crystals at the CHESS synchrotron at Cornell and processed using only fully recorded reflections during each 1° rotation.[2] Both native data sets were merged to produce the data set used in refinement (R_{merge} = 6.3%, 92.2% overall completeness, 79.5% complete between 2.5 and 2.4 Å). Refinement was done using the program XPLOR (Brünger et al., 1987; Brünger, 1990; Engh & Huber, 1992). In the initial rounds, the model was manually adjusted on the basis of σ_A-weighted, phase-combined electron density maps (Read, 1986). Prior to the last refinement rounds the native data set was corrected for the observed anisotropy, yielding a 22-Å^2 difference in B-factor between the c and the a/b directions. Although this correction resulted in only a slight decrease of the crystallographic R-factor (1.5%), the quality of the electron density maps was considerably improved in terms of connectivity and sharpness. A portion of the final $2F_o - F_c$ map is shown in Figure 1.

RESULTS AND DISCUSSION

The present model of the extracellular domain of TF consists of residues 4–210 together with 65 water molecules. In addition to the termini, two loops cannot be built with confidence (residues 84–90 and 119–121) and are omitted from the model, while one further loop shows poor electron density (residues 161–163). The crystallographic R-factor is 22.4% (9303 reflections with $F > 0$ between 10 and 2.4 Å), and deviations from ideal bond lengths and angles are 0.016 Å and 2.0°, respectively. The average isotropic temperature factor is 39 Å^2, with a 1.9-Å^2 root-mean-square difference for bonded atoms. The only residue outside the "allowed" region of the Ramachandran plot is Asn137, which is involved in close crystal packing contacts.

TF consists of two compact domains with identical connectivity (residues 1–103 and 104–210, respectively). Each domain is folded into a β-sandwich containing one four-

[2] The computer program DENZO, for the reduction of oscillation images, was written by Z. Otwinowski (Yale University); we used a version with graphics capabilities added by Wladek Minor (Purdue University). SCALEPACK, a program for scaling of oscillation data, was written by Z. Otwinowski.

FIGURE 2: Ribbon representation of the structure of the extracellular domain of human tissue factor generated with the program MOLSCRIPT (Kraulis, 1991). The β-strands in the seven-stranded β-sandwich domains are labeled following the established convention for the fibronectin type III fold (Baron et al., 1992; Leahy et al., 1992).

stranded and one three-stranded sheet (Figure 2), with fibronectin type III topology (Baron et al., 1992; Leahy et al., 1992). A tryptophan (Trp25 in TF) which is strictly conserved throughout the cytokine receptor superfamily is buried in the core of the N-terminal sandwich. One disulfide bridge is also conserved; it is located between strands C′ and E of the N-terminal domain. In TF, a second disulfide bridge is present between strands F and G at the solvent-accessible face of the C-terminal domain. The surface of TF shows two distinctive patterns of side-chain distributions, both located in the N-terminal domain. The first cluster is found at the solvent-exposed side of the four-stranded β-sheet and is formed by six aromatic side chains (Trp45, Phe50, Phe76, Tyr51, Tyr78, and Tyr94). The second is located at the solvent-exposed face of the three-stranded sheet and consists of nine charged residues (Glu24, Glu26, Glu56, Asp54, Asp58, Asp61, Lys15, Lys20, and Lys28). The overall significance of these clusters remains unclear, although two of the residues in the charge cluster have functional importance (below).

The two-domain organization and the domain topology of TF are similar to those of the extracellular part of the growth hormone receptor (Figure 3) (De Vos et al., 1992). In contrast to this receptor, however, where the tertiary structure of the N-terminal domain differs slightly from the fibronectin type III module, both domains of TF have the canonical fibronectin type III fold. Additional differences between TF and the growth hormone receptor occur in the loop regions connecting the β-strands. An insertion of nine residues, whose sequence is highly conserved in the human, mouse, and rabbit proteins, is found between strands B and C of the C-terminal domain of TF. This segment, together with some of the preceding residues, forms a short two-stranded antiparallel β-ribbon followed by a short α-helix (Figure 2). A second short α-helical segment not present in the growth hormone receptor is part of the segment linking strands E and F in the N-terminal domain. Residues from both of these regions are involved in contacts across the domain–domain interface. The conformation of the linker segment connecting the domains is very similar in TF and the growth hormone receptor. In TF the linker consists of a short α-helical turn (3_{10}-turn in growth hormone receptor) followed by a segment in extended conformation immediately preceding strand A of the C-terminal domain.

Superimposing the C-terminal domain of TF on that of the growth hormone receptor shows that the orientation of the N-terminal domain differs dramatically in both structures (Figure 3). The angle between the two domains is about 125° in TF compared to 80° in the growth hormone receptor; in addition, there is a difference of about 15° when looking down the axis of the C-terminal sandwich. These changes in orientation result from large differences in the interface between the domains. Although the total area buried in the domain–domain interface is similar in both proteins [about 600 Å^2; calculated with XPLOR (Brünger, 1990); probe radius 1.4 Å], in contrast to the growth hormone receptor the hydrophobic core in TF is continuous throughout the interface. As a consequence, the solvent accessibility and the ability to contribute to ligand binding of residues within or next to the interface differ significantly between TF and the growth hormone receptor. In the latter, the loop connecting strands A and B of the N-terminal domain contains Arg43, whose side chain makes a major contribution to hormone binding (De Vos et al., 1992; T. Clackson and J. Wells, personal communication). In TF, the side chains of the residues in the equivalent loop are mostly buried within the interface. For example, Phe19, which is the equivalent of Arg43 of the growth hormone receptor, fits in a pocket formed by the side chains of Val64 and Val67 of the N-terminal domain, Pro102, Thr106, and Tyr103 of the linker, and Thr132, Val134, Val146, and Phe147 of the C-terminal domain. The most important binding determinants of the human growth hormone receptor are Trp104 and Trp169 (De Vos et al., 1992; Bass et al., 1991; T. Clackson and J. Wells, personal communication), which are positioned close together in space. In TF, the residue homologous to Trp104 is Lys68, which is distant from the equivalent of Trp169 due to the changes in the domain interface region including the presence of the nine-residue insertion in the C-terminal domain.

TF is only the second example of a repeat of standard fibronectin type III modules for which the three-dimensional structure is known, the other case being the tandem type III domains from neuroglian (Huber et al., 1994). Comparison of these structures shows that the interface region and conformation of the linker segment differ considerably, with the result that the relative domain–domain orientations are very different. Similar variability in domain interface and orientation (Campbell & Spitzfaden, 1994) is observed in structures containing a repeat of immunoglobulin-like domains such as CD2 (Jones et al., 1992) and CD4 (Ryu et al., 1990; Wang et al., 1990). It is noteworthy that a helical conformation of the linker segment has thus far only been observed for TF, the growth hormone receptor (De Vos et al., 1992), and the prolactin receptor (W. Somers, M. Ultsch, A. M. de Vos, and A. A. Kossiakoff, unpublished results), raising the possibility that this conformation is a unique feature of the cytokine receptor superfamily.

Alanine-scanning mutagenesis (Wells, 1991) of TF, initially targeting proposed loop segments based on the structure of the growth hormone receptor, has been used to probe the determinants of TF cofactor function (Ruf et al., 1994).[3] Only

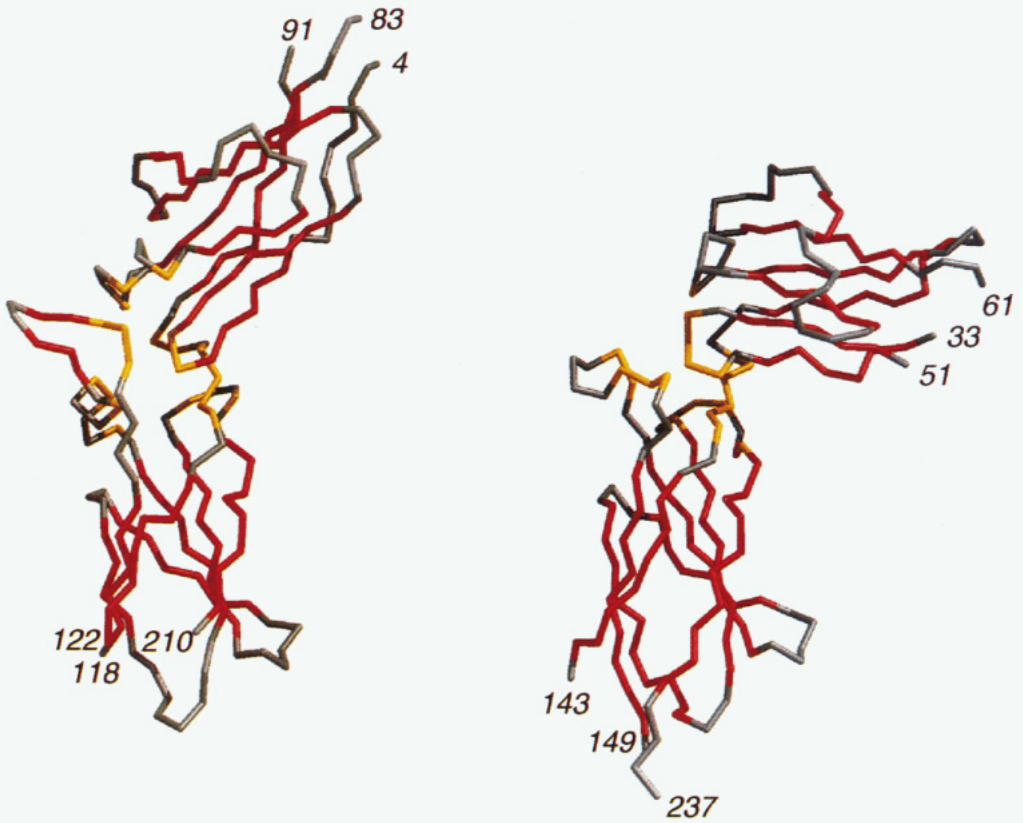

FIGURE 3: Main-chain representation of the extracellular domain of TF (left) and the growth hormone receptor (right), generated using the program MIDAS (Ferrin et al., 1988). Loops are shown in gray and β-strands in red. Residues that are buried in the interface are colored yellow. The orientation depicted here was derived from a superposition of the C-terminal domains, giving an rms difference between 65 equivalent Cα positions of 1.2 Å. Superimposing the N-terminal domains yields an rms difference of 1.6 Å (57 Cα positions), whereas the two domains of TF can be superimposed to each other with an rms difference of 1.4 Å (58 Cα positions) [program OVERLAY (Kabsch, 1978), distance cutoff of 3 Å].

a small number of residues make a significant contribution to the binding of FVIIa. For solvent-exposed residues, alanine substitution of Lys20, Ile22, Asp58, or Phe140 resulted in a greater than 10-fold increase in the apparent dissociation constant (K_{Dapp}) for FVIIa binding, while mutation of Arg135 resulted in a 7.4-fold increase in K_{Dapp} (Ruf et al., 1994). All other substitutions had a less than 5-fold effect on FVIIa binding with most being less than 2-fold. Lys20 and Ile22 are situated in the central region of strand B of the N-terminal domain, next to Asp58 in the adjacent strand E (Figure 4A). The Cα atoms of these residues form a triangle with edges 6.9, 8.0, and 4.2 Å long, located near the domain–domain interface at its concave side. Arg135 and Phe140 are situated in the antiparallel β-ribbon portion of the long insertion formed between strands B and C of the C-terminal domain, with the Cα atom of Phe140 13.1 Å from the Cα of Lys20. Contrary to both the antigen binding sites on antibodies (Davies et al., 1990; Kelley & O'Connell, 1993) and the ligand binding site on the growth hormone receptor (De Vos et al., 1992; Bass et al., 1991; T. Clackson and J. Wells, personal communication), where the binding determinants reside on loops, in TF the important residues for FVIIa binding are contributed by more rigid β-strands.

An additional set of substitutions effect a significant reduction in the coagulant function of TF without an effect on FVIIa binding (Ruf et al., 1994). Coagulant function was reduced by at least 50% when mutations were introduced in any of the segments 16–19, 103–106, 157–166, or 199–201 or when Tyr71 was mutated to alanine. Inspection of the structure suggests that, except for the segment from 157 to 166, most of these residues are required for the structural integrity of TF. The side chain of Tyr157 is buried within the β-sandwich, but those of residues 158–166 are exposed into the solvent. A double mutant TF having lysine residues 165 and 166 replaced with alanine displays a much reduced cofactor function in the activation of factor X (Roy et al., 1991) despite binding FVIIa with wild-type affinity. This defect is not observed for peptide substrates and involves an increase in the K_M for factor X activation (Ruf et al., 1992), suggesting that these residues contribute to protein substrate recognition by the TF·FVIIa complex. The 157–166 portion of TF is located next to the C-terminus of the extracellular domain and thus could modulate activity through interactions with phospholipid (Roy et al., 1991). However, the defect in cofactor function for the Lys165, Lys166 double mutant is also observed for both soluble TF (Kelley, unpublished results) and full-length TF in the absence of phospholipid (Ruf et al., 1992). The Cα to Cα distance between Lys20 and Lys165 is about 33 Å. It has been proposed that the Gla and EGF domains of FVII provide the interactive region for binding to the N-terminal domain of TF (Toomey et al., 1991; Kazama et al., 1993). If this region corresponds to the site shown in Figure 4A, given the size of FVII (50 kDa), its protease domain should be able to contact lysines 165 and 166 of TF in order to maintain the binding site on FVII for factor X. Alternatively, direct contacts between factor X and the 157–166 segment of TF may be required to properly form the ternary complex.

Mapping of the respective binding determinants on TF and on the growth hormone receptor reveals a dramatic difference

[3] We have observed effects of TF mutations on FVIIa affinity similar to those of Ruf et al. (1994) by using a Pharmacia BIAcore system to measure binding constants. A minor exception is that we detect smaller K_D changes for the Arg135 and Phe140 mutations; we attribute this to differences in the assay methods employed.

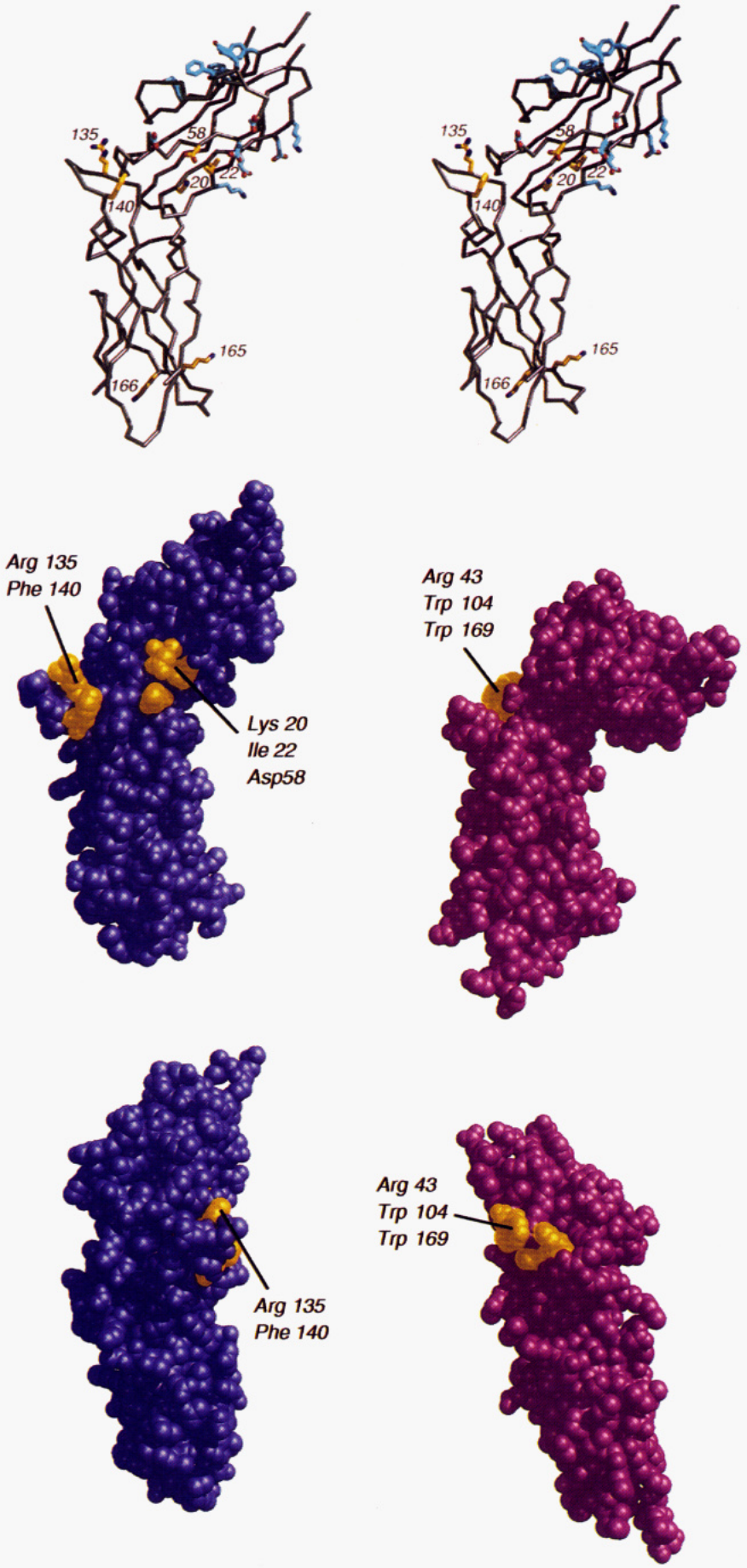

FIGURE 4: (A, top) Stereo Cα representation of human TF. Residues important for binding of FVII are shown in yellow. Clusters of aromatic and charged residues are indicated in light blue, with the latter including Lys20 and Asp58. (B, middle, and C, bottom) Space-filling models of TF (in purple) and the growth hormone receptor (burgundy) with residues important for ligand binding colored yellow. (B) and (C) are perpendicular views, with the orientation in (B) identical to that in Figure 3.

in the location of the ligand-binding sites. As indicated by the structural comparisons depicted in Figure 4B,C, the FVIIa binding site on TF, while near the domain–domain interface, is located on the opposite side of the cytokine receptor fold relative to the ligand-binding site on the growth hormone receptor. This is a consequence of the differences in domain–domain interactions that bury some of the residues of TF that are located in exposed loops in the growth hormone receptor. With regard to the cytokine receptor superfamily, the similarities in structure both among the receptor extracellular domains and among the ligands for most of these receptors (De Vos & Kossiakoff, 1992; Wells & de Vos, 1993; Sprang & Bazan, 1993) (but not for TF) suggest that the location of the ligand-binding site at the interface of the N- and C-terminal domains of the cytokine receptor module be conserved throughout the superfamily. The present structure shows that the mutational data available for TF are consistent with this hypothesis. However, the structure also shows that TF does not use the residues equivalent to the binding determinants in the growth hormone receptor but instead amino acids that are nearby in the sequence. Structural data on the prolactin receptor (W. Somers, M. Ultsch, A. M. de Vos, and A. A. Kossiakoff, unpublished results) as well as mutational data on other receptors (Imler et al., 1992; Wang et al., 1992; Yawata et al., 1993) support the notion that their binding sites are more similar to that of the growth hormone receptor than to that of TF. However, even if TF should represent a unique case, its example shows that the design and interpretation of mutagenesis experiments directed at the identification of the binding sites of receptors within the cytokine superfamily still require considerable caution in the absence of specific structural data.

ACKNOWLEDGMENT

At Genentech, Inc., we thank the organic chemistry department for oligonucleotide synthesis, Han Chen for fermentations, and John Stults for mass spectrometry. We acknowledge Bob Lazarus for discussions and advice in formulating this research. We are grateful to Bill Miller, Tom Irving, and Marian Szebenyi at CHESS for advice on data collection and processing and to Wladek Minor (Purdue University) for a temporary license for DENZO and SCALEPACK. From Genentech, Inc., Will Somers, Theresa Gamble, Mike Randal, and Axel Scheidig helped with data collections at CHESS, and Tony Kossiakoff gave useful comments on the manuscript. We thank Pamela Bjorkman (California Institute of Technology) for giving us the coordinates of the tandem fibronectin III structure.

REFERENCES

Baron, M., Main, A. L., Driscoll, P. C., Mardon, H. J., Boyd, J., & Campbell, I. D. (1992) *Biochemistry 31*, 2068.

Bass, S. H., Mulkerrin, M. M., & Wells, J. A. (1991) *Proc. Natl. Acad. Sci. U.S.A. 88*, 4498.

Bazan, J. F. (1990) *Proc. Natl. Acad. Sci. U.S.A. 87*, 6934.

Bom, V. J. J., & Bertina, R. M. (1990) *Biochem. J. 265*, 327.

Boys, C. W. G., Miller, A., Harlos, K., Martin, D. M. A., Tuddenham, E. G. D., & O'Brien, D. P. (1993) *J. Mol. Biol. 234*, 1263.

Brünger, A. T. (1990) *XPLOR manual*, Yale University Press, New Haven, CT.

Brünger, A. T., Kuriyan, J., & Karplus, M. (1987) *Science 235*, 458.

Campbell, I. D., & Spitzfaden, C. (1994) *Structure 2*, 333.

Davie, E. W., Fujikawa, K., & Kisiel, W. (1991) *Biochemistry 30*, 10363.

Davies, D. R., Padlan, E. A., & Sheriff, S. (1990) *Annu. Rev. Biochem. 59*, 439.

De Vos, A. M., & Kossiakoff, A. A. (1992) *Curr. Opin. Struct. Biol. 2*, 852.

De Vos, A. M., Ultsch, M., & Kossiakoff, A. A. (1992) *Science 255*, 306.

Engh, R. A., & Huber, R. (1992) *Acta Crystallogr. A47*, 392.

Ferrin, T. E., Huang, C. L., Jarvis, L. E., & Langridge, R. (1988) *J. Mol. Graphics 6*, 13.

Gregory, S. A., Morrissey, J. H., & Edgington, T. S. (1989) *Mol. Cell. Biol. 9*, 2752.

Huber, A. H., Wang, Y.-E., Bieber, A. J., & Bjorkman, P. J. (1994) *Neuron 12*, 717.

Imler, J. L., Miyajima, A., & Zurawski, G. (1992) *EMBO J. 11*, 2047.

Jones, A. T. (1978) *J. Appl. Crystallogr. 11*, 268.

Jones, E. Y., Davis, S. J., Williams, A. F., Harlos, K., & Stuart, D. I. (1992) *Nature 360*, 232.

Kabsch, W. (1978) *Acta Crystallogr. A34*, 827.

Kabsch, W. (1988) *J. Appl. Crystallogr. 21*, 916.

Kazama, Y., Pastuszyn, A., Wildgoose, P., Hamamoto, T., & Kisiel, W. (1993) *J. Biol. Chem. 268*, 16231.

Kelley, R. F., & O'Connell, M. P. (1993) *Biochemistry 32*, 6828.

Kraulis, P. J. (1991) *J. Appl. Crystallogr. 24*, 946.

Lawson, J. H., Butenas, S., & Mann, K. G. (1992) *J. Biol. Chem. 267*, 4834.

Leahy, D. J., Hendrickson, W. A., Aukhil, I., & Erickson, H. P. (1992) *Science 257*, 987.

Messerschmidt, A., & Pflugrath, J. W. (1987) *J. Appl. Crystallogr. 20*, 306.

Morrissey, J. H., Fakhrai, H., & Edgington, T. S. (1987) *Cell 50*, 129.

Nakagaki, T., Foster, D. C., Berkner, K. L., & Kisiel, W. (1991) *Biochemistry 30*, 10819.

Nemerson, Y. (1988) *Blood 71*, 1.

Nemerson, Y., & Repke, D. (1985) *Thromb. Res. 40*, 351.

Neuenschwander, P. F., & Morrissey, J. H. (1994) *J. Biol. Chem. 269*, 8007.

Neuenschwander, P. F., Fiore, M. M., & Morrissey, J. H. (1993) *J. Biol. Chem. 268*, 21489.

Pawashe, A. B., Golino, P., Ambrosio, G., Migliaccio, F., Ragni, M., Pascucci, I., Chiariello, M., Bach, R., Garen, A., Koningsberg, W. K., & Ezekowitz, M. D. (1994) *Circ. Res. 74*, 56.

Read, R. J. (1986) *Acta Crystallogr. A42*, 140.

Roy, S., Hass, P. E., Bourell, J. H., Henzel, W. J., & Vehar, G. A. (1991) *J. Biol. Chem. 266*, 22063.

Ruf, W., & Edgington, T. S. (1994) *FASEB J. 8*, 385.

Ruf, W., Miles, D. J., Rehemtulla, A., & Edgington, T. S. (1992) *J. Biol. Chem. 267*, 6375.

Ruf, W., Schullek, J. R., Stone, M. J., & Edgington, T. S. (1994) *Biochemistry 33*, 1565.

Ryu, S.-E., Kwong, P. D., Truneh, A., Porter, T. G., Arthos, J., Rosenberg, M., Dai, X., Xuong, N.-H., Axel, R., Sweet, R. W., & Hendrickson, W. A. (1990) *Nature 348*, 426.

Scarpati, E. M., Wen, D., Broze, G. J., Jr., Miletich, J. P., Flandermeyer, R. R., Siegel, N. R., & Sadler, J. E. (1987) *Biochemistry 26*, 5324.

Spicer, E. K., Horton, R., Bloem, L., Bach, R., Williams, K. R., Guha, A., Kraus, J., Lin, T. C., Nemerson, Y., & Konigsberg, W. K. (1987) *Proc. Natl. Acad. Sci. U.S.A. 84*, 5148.

Sprang, S. R., & Bazan, J. F. (1993) *Curr. Opin. Struct. Biol. 3*, 815.

Steigemann, W. (1974) Thesis, Technische Universitat, München.

Taylor, F. B., Jr., Chang, A., Ruf, W., Morrissey, J. H., Hinshaw, L., Catlett, R., Blick, K., & Edgington, T. S. (1991) *Circ. Shock 33*, 127.

Terwilliger, T., Kim, S.-H., & Eisenberg, D. (1987) *Acta Crystallogr. A43*, 1.

Toomey, J. R., Smith, K. J., & Stafford, D. W. (1991) *J. Biol. Chem. 266*, 19198.

Wang, B. C. (1985) *Methods Enzymol. 115*, 90.
Wang, H., Ogorochi, T., Arai, K., & Miyajima, A. (1992) *J. Biol. Chem. 267*, 979.
Wang, J., Yan, Y., Garrett, T. P. J., Liu, J., Rodgers, D. W., Garlick, R. L., Tarr, G. E., Husain, Y., Reinherz, E. L., & Harrison, S. C. (1990) *Nature 348*, 418.
Warr, T. A., Rao, L. V. M., & Rapaport, S. I. (1990) *Blood 75*, 1481.
Wells, J. A. (1991) *Methods Enzymol. 153*, 3.
Wells J. A., & de Vos, A. M. (1993) *Annu. Rev. Biophys. Biomol. Struct. 22*, 329.
Wilcox, J. N., Smith, K. M., Schwartz, S. M., & Gordon, D. (1989) *Proc. Natl. Acad. Sci. U.S.A. 86*, 2839.
Yawata, H., Yasukawa, K., Natsuka, S., Murakami, M., Yamasaki, K., Hibi, M., Taga, T., & Kishimoto, T. (1993) *EMBO J. 12*, 1705.